Assessment of Three-phase Induction Motor Dynamic Regimes Following Ecosystem Patterns

NIKOS E. MASTORAKIS [1] CORNELIA A. BULUCEA [2] DORU A. NICOLA [2]
[1] Military Institutes of University Education, Hellenic Naval Academy
GREECE
[2] Faculty of Electromechanical and Environmental Engineering, University of Craiova
ROMANIA
mastorakis4567@gmail.com, abulucea@gmail.com, dnicola@em.ucv.ro

Abstract: Within the present industrial society the humans further challenges are doubtless related to a sustainable industrial metabolism, integrating industrial activity into ecological systems. An approach of technical systems and ecological systems as parts of the same system, the industrial ecosystem, could provide a holistic view of the interactions and symbiosis interrelationships among human activities, technical systems operation and ecological processes. In this study are pointed the ecosystem key-features suitable for the electrically driven transportation systems analysis. By modeling the electrical traction machines dynamic regimes according to an industrial ecosystem pattern, one could attempt to minimize the environmental impacts and optimize the efficiency of energy use within the transportation systems operation.

Key-Words: Dynamic Regimes, Induction Machine, Industrial Ecosystem, Transportation System

1 Introduction

Industrial Ecology as a science is defined within the framework of Sustainable Development [1], and considers the technical systems created by humans and the ecological systems of Nature as parts of the same system, the *industrial ecosystem*, that can exists on a multitude of temporal and spatial scales. Within the framework of sustainability, Industrial Ecology implies a new picture of energy and matter conversion systems, and aims in designing the technical systems more like ecosystems [2]. It means that the laws of the Universe should be used in assessing the viability of the human technical applications according to the ecosystems models.

On a broader front, an utmost human world priority should be the improvement of public transportation systems. The merit of an electric transportation system is based not only on technical performance, safety, energy efficiency, societal and economic acceptance and but also on environmental impacts limitation and exergy efficiency increase.

This study aims to find the analogies between the ecosystems and electrical transportation systems regarding the key features of structure and function.

We are taking into consideration the electric trains supplied from a d.c. contact line equipped with three-phase induction motors (having squirrel cage rotors) and variable voltage and frequency inverters [3]. Since the electric driving systems with static converters and traction induction motors are used, by an appropriate control, with the same electrical machines there can be realized both the traction regime and the electric braking regime of the electric traction vehicles [4].

One could start from the key-feature setting that *an industrial ecosystem does not have single equilibrium point, but the system move among multiple stable states* [5], [6]. *It means that every steady-state operation regime of the transportation system can be seen as a stable state of an analogue ecosystem*. In the power electrical chain there are many types of energy conversion, and the induction motors produce the final electromechanical conversion, making thus possible the vehicle movement. Hence, an analysis of the electric machine behavior at variable frequency operation is one of the compulsory steps in the achievement of an optimum control of the electric train [7].

2 Induction Machine Operation at Variable Frequency with Controlled Flux

The vehicle regulation speed is performed looking at the static converter and electric machine as an assembly. The traction motors speed regulation is based on stator voltage and frequency variation, so

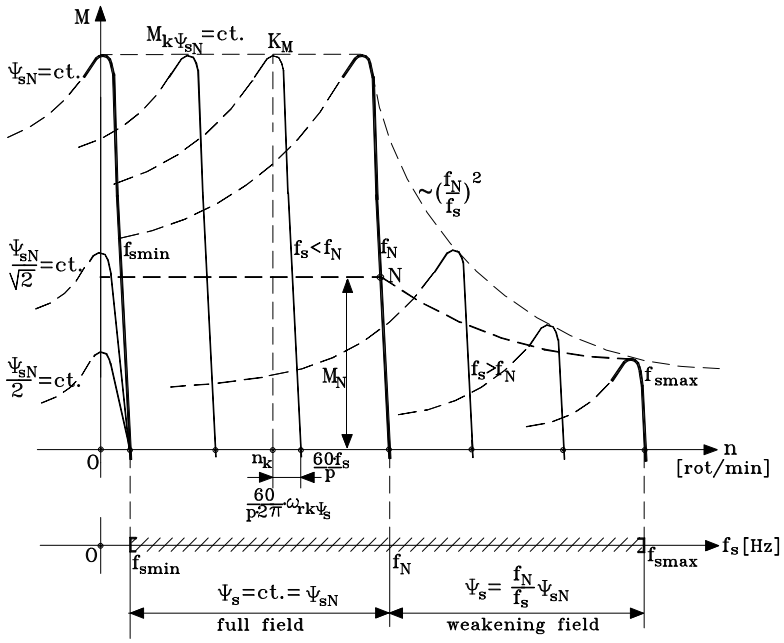

Fig.1 Mechanical characteristics M=f(n) for different stator frequency f_s values

that, in the aim of a *high exergy efficiency, an utmost requirement of the train control system is concerning the passing of operation equilibrium point from one mechanical characteristic to another*. Step by step, one could present a new point of view regarding the analysis of transportation system behavior in dynamic regimes.

In the range of the frequencies lower than rated frequency $f_s < f_N$, in order to ensure a constant level of inductor machine stator flux $\Psi_s = \Psi_{sN}$, at the same time have to be modified the frequency f_s and the supply r.m.s. voltage U_s.

In case of induction machine supplied from a variable frequency voltage source when rated speed is reached (induction motor supplied at U_N and f_N) the further speed increase will be possible only by increasing the stator frequency magnitude over the rated frequency $f_s>f_N$. It must be emphasized that because of both converters voltage restriction and induction machine windings insulation considerations, the stator voltage will be limited and maintained at constant magnitude $U_s=U_N$ on all high frequency domain, and the induction machine will operate in weakened flux conditions [7]. From exergetic viewpoint it must be notified that, because the stator flux and pulsation are into a inverse proportionality relation $\Psi_s=U_N/\omega_s$, the machine torque capability will be strongly affected.

As conclusion at this point, one could highlight that the induction machine supplied from a variable frequency and voltage source will operate with full field $\psi_s = \psi_{Sn}$ = ct. in the low frequencies range $f_s \le f_N$ and with weaken field ($\psi_s<\psi_{Sn}$) in the increased frequencies domain $f_s > f_N$ (when the supply r.m.s. voltage remains constant $U_s=U_N$=ct.).

When and how the movement of machine operation point from a mechanical characteristic to another is performed means , in fact, to know how the control of the electrically driven system must be proceeded.

The operation at variable frequency with controlled flux is performed to induction motors in electrically driven systems with vectorial control [8]. The vectorial regulation and control method is based on space phasor theory, taking into account the control of (both) the induction machine flux and electromagnetic torque M. As principle, the stator current space phasor is decomposed in two perpendicular components (a flux component and a torque component) which are separately controlled. In this paper it is considered the permanent harmonics regime of variable frequency operation with controlled stator flux. It must be noted that, in the theoretical achievements, it will be taken into account the induction machine with constant parameters, without iron exergy losses or saturation.

3 Modeling of Three-phase Induction Machine in Dynamic Regimes

Basicly, by the *induction machines modeling* one could understand the use of *conventional representations* (geometric constructions, electrical circuits, structural diagrams etc.) to describe the behavior (or for the simulation) of various operation states or regimes [9]. The classic models, meaning the equivalent electric schemes and the phasor diagrams of the induction motors, could be considered only in the permanent regimes operation, when all the state-quantities have a sinusoidal variation in time. In dynamic regimes, they lose their validity and other models should be developed [10].

Physically, dynamic regimes of induction motors are characterized by the variation in time of both "electromagnetic status" (the currents and fluxes) and "mechanical status" (movement) of the rotors. Qualitatively, the dynamic phenomena of electromagnetic nature in the induction machines are fast and are developing with small time-constant (usually, between 1 and 100 ms). In contrast, the dynamic phenomena of mechanical nature match the acceleration and / or deceleration of rotating mass and held relatively the large time-constant (usually, between 100 ms and 0.5 s).

Mathematically, the processes dynamics (both electromagnetic and mechanical) of induction motors are described by differential equations which, in most cases, are nonlinear. Based on the *mathematical model equations*, in this paper will be presented the *structural diagrams method*, as a *modeling method of induction motors in dynamic regimes*. Among others, the benefit derived from the easily conversion of structural diagrams in Matlab-Simulink implementations.

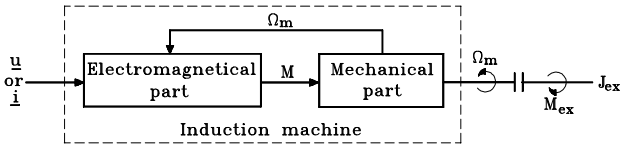

Fig.2 Three-phase induction motor modeling
($\omega_m = p \cdot \Omega_m$; p = poles pairs number)

Regardless of the application, induction motors are complex systems, which perform an electromechanical conversion of energy. Concretely, they receive "at the terminals" the electric energy $W_{1(el)}$ and after covering the "losses" (in fact, energy flows, about 8-20% of the energy received) they provide "at the axle" the useful mechanical energy $W_{2(mec)}$. Therefore, for modeling, it is necessary an overview of the electric motor system from terminals towards axle and a formal split into an "electromagnetic part and a" mechanical part", the two subsystems having been interconnected, exactly as it is shown in Fig.2.

The idea of imaginary decomposing of induction motor in the two parts makes possible the picture of integrating it within the two systems that need to be controlled . Thus, the *electromagnetic part model* coupled with the *power supply side model* ("in current" or "in voltage") represents the *system controlled by electrical methods*. Absolutely similar, the *mechanical part model* coupled with the *mechanical transmission model* will form the *mechanically controlled system* (by mechanical methods).

Physically, *the mechanical part* of the induction motor will contain only the inertia of the rotating masses, and it is governed by the laws of classical mechanics.

In the diagram of the induction motor electromagnetic part modeling , *the input quantity* is either the space phasor $\underline{u}_s$ (supplying "in voltage") or the space phasor $\underline{i}_s$ (supplying "in current"). As *output quantity* is resulting the electromagnetic torque M. Both magnetic fluxes, and rotor and stator currents are internal quantities, and do not appear explicitly in the modeling diagram of Fig.2.

In the diagram of the induction motor mechanical part modeling, *the input quantity* is the electromagnetic torque M. As *output quantities* are resulting the rotor mechanical angular speed Ω_m and the useful torque M_2 transmitted to the axle.

On the other hand, both the electromagnetic torque M, and the mechanical pulsation ω_m (or the rotor angular speed Ω_m , with $\omega_m = p \cdot \Omega_m$) are *direct and inverse interaction quantities* between the two fundamental parts of the induction motor. Based on this idea, further on, one could construct the *structural diagrams* of the induction motor electromagnetic part.

3.1 Modeling of Electromagnetic Subsystem of Three-phase Induction Motors Supplied by Voltage Sources

One could consider the three-phase induction motors with the stator supplied by a phase voltages system as the form u_{sa}, , u_{sb} , u_{sc} either from the electric network (with constant frequency $f_s = 50$ *Hz)* or from a three-phase voltage static convert with variable frequency f_s. Whatever is the three-phase voltages supply source, for describing the dynamic electromagnetic phenomena the *space phasors method* will be applied.

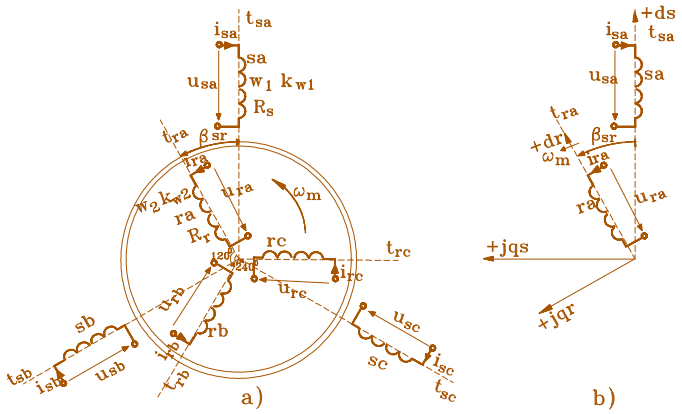

Fig.3 Three-phase induction machine: a) representation b) referentials and reference phases

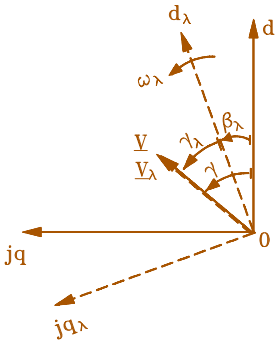

Fig.4 General referential (d_λ, jq_λ, t_λ)

For the three-phase induction machine (with electrical and magnetic symmetry, Fig.3) one could consider the equations written with the space phasors related to the general referential *(d_λ, jq_λ, t)* that is rotating with the angular speed ω_λ (Fig.4), and with the rotor magnitudes related to stator. These equations will create, basicly, *the mathematical model of electromagnetic subsystem of the three-phase induction motor*. In the case of *linear electromagnetic model* (under the assumption of magnetic unsaturated machine) the mathematical model equations are written as follows:

$$\underline{u}_{s\lambda} = R_s \cdot \underline{i}_{s\lambda} + \frac{d\underline{\psi}_{s\lambda}}{dt} + j \cdot \omega_\lambda \cdot \underline{\psi}_{s\lambda}$$

$$\underline{u}'_{r\lambda} = R'_r \cdot \underline{i}'_{r\lambda} + \frac{d\underline{\psi}'_{r\lambda}}{dt} + j \cdot (\omega_\lambda - \omega_m) \cdot \underline{\psi}'_{r\lambda}$$

$$\underline{\psi}_{s\lambda} = L_s \cdot \underline{i}_{s\lambda} + L_{su} \cdot \underline{i}'_{r\lambda} \qquad (1)$$

$$\underline{\psi}'_{r\lambda} = L_{su} \cdot \underline{i}_{s\lambda} + L'_r \cdot \underline{i}'_{r\lambda}$$

$$M = \frac{3}{2} \cdot p \cdot Im\{\underline{i}_{s\lambda} \cdot \underline{\psi}^*_{s\lambda}\}; \quad \omega_m = p \cdot \Omega_m$$

where: $\underline{u}_{s\lambda}$ is the stator voltage space phasor; $\underline{u}'_{r\lambda}$ is the rotor voltage space phasor; $\underline{i}_{s\lambda}$ is the stator current space phasor; $\underline{i}_{r\lambda}$' is the rotor current space phasor; $\underline{\Psi}_{s\lambda}$ is the stator flux space phasor; $\underline{\Psi}_{r\lambda}$' is the rotor flux space phasor; L_{su} is the magnetizing inductance; L_s is the stator inductance; L_r' is the rotor inductance; p is the number of pole pairs; R_s is the stator resistance; R_r' is the rotor resistance, and M is the electromagnetic torque.

Similarly, in the case of *non-linear electromagnetic model*, taking into account the ferromagnetic core magnetizing characteristic $\Phi_u = f(i_\mu)$ the mathematical model will be written as below:

$$\underline{u}_{s\lambda} = R_s \cdot \underline{i}_{s\lambda} + \frac{d\underline{\psi}_{s\lambda}}{dt} + j \cdot \omega_\lambda \cdot \underline{\psi}_{s\lambda}$$

$$\underline{u}'_{r\lambda} = R_{r'} \cdot \underline{i}'_{r\lambda} + \frac{d\underline{\psi}'_{r\lambda}}{dt} + j \cdot (\omega_\lambda - \omega_m) \cdot \underline{\psi}_{r'\lambda}$$

$$\underline{\psi}_{s\lambda} = L_{s\sigma} \cdot \underline{i}_{s\lambda} + \underline{\psi}_{u\lambda}$$

$$\underline{\psi}'_{r\lambda} = L'_{r\sigma} \cdot \underline{i}'_{r\lambda} + \underline{\psi}_{u\lambda} \qquad (2)$$

$$|\underline{\psi}_{u\lambda}| = \psi_u \; ; \qquad \psi_u = \psi_u(i_\mu)$$

$$\underline{i}_{s\lambda} + \underline{i}'_{r\lambda} = \underline{i}_{\mu\lambda} \; ; \quad |\underline{i}_{\mu\lambda}| = i_\mu$$

$$M = \frac{3}{2} \cdot p \cdot Im\{\underline{i}_{s\lambda} \cdot \underline{\psi}^*_{s\lambda}\}; \quad \omega_m = p \cdot \Omega_m$$

It must be noticed that in all equations as above the space phasors $\underline{u}_{s\lambda}$, $\underline{i}_{s\lambda}$, $\underline{i}'_{r\lambda}$, $\underline{\Psi}_{s\lambda}$, $\underline{\Psi}'_{r\lambda}$ are related to the general referential *(d_λ,jq_λ,t)* rotating with the angular speed $\omega_\lambda = d\beta_\lambda/dt$. Further on, for the electromagnetic part can be achieved structural models with the space phasors written in various referentials, two of them having been important: *1)* the fixed referential, related to stator (when $\omega_\lambda = 0$) and *2)* the referential rotating with the synchronism speed (when $\omega_\lambda = \omega_s$). For each of them can be performed both the linear and nonlinear models for the three-phase induction motors (with squirrel cage rotor, when $\underline{u}'_{r\lambda} = 0$).

3.2 Patterns and Structural Diagrams with Space Phasors in Fixed Coordinates Related to Stator

For this case the common referential *(d_λ, jq_λ, t)* is a fixed one, related to stator (meaning $\omega_\lambda = 0$), and having the real axis d_λ over-positioned to the magnetic axis of the reference winding "*sa*". Consequently, the imaginary axis jq_λ will be rotated in direct sense with $90^o el$. If u_{sa}, u_{sb}, u_{sc} are the instantaneous values of the phase stator voltages, then, in fixed coordinates, the voltage space phasor $\underline{u}_{ss}$ (as input quantity) will be:

$$\underline{u}_{ss} = \frac{2}{3} \cdot (u_{sa} + a \cdot u_{sb} + a^2 \cdot u_{sc}) \qquad (3)$$

where, obviously, $a = e^{j\frac{2\pi}{3}}$ and $a^2 = e^{j\frac{4\pi}{3}}$ are the complex operators of rotation with $2\pi/3$ and $4\pi/3$ el.rad.., respectively.

In a inverse sense, if $\underline{i}_{ss}$ represents the stator currents space phasor (as output quantity), then the instantaneous values of the phase currents i_{sa}, i_{sb}, i_{sc} will be:

$$i_{sa} = Re\{\underline{i}_{ss}\}; i_{sb} = Re\{a^{-1} \cdot \underline{i}_{ss}\}; i_{sc} = Re\{a^{-2} \cdot \underline{i}_{ss}\} \quad (4)$$

Adequately to these transformation relations, in Fig.5, as the form of structural diagrams, both the direct and inverse transformings are represented.

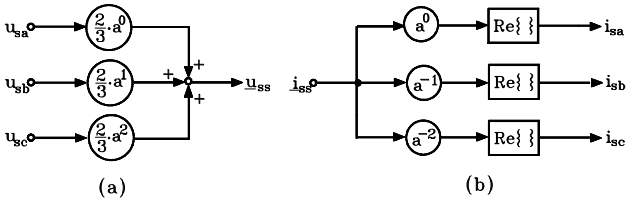

Fig.5 Models of direct (a) and inverse (b) transformings in fixed coordinates, as structural diagrams form

Consequently, the diagrams represented in Fig.5 could be coupled at the input (scheme "a") and at the output (scheme "b") of the structural diagrams of the electromagnetic part of the three-phase induction machine supplied in voltage, described by the space phasors in fixed coordinates related to the stator.

3.2.1 Linear Electromagnetic Pattern

In this case the ferromagnetic core is unsaturated, and the electromagnetic part equations are established under the assumptions $\omega_\lambda = 0$, $u'_{r\lambda} = 0$, $\lambda = s$:

$$\underline{u}_{ss} = R_s \cdot \underline{i}_{ss} + \frac{d\underline{\psi}_{ss}}{dt} \quad (5a)$$

$$0 = R'_r \cdot \underline{i}'_{rs} + \frac{d\underline{\psi}'_{rs}}{dt} - j \cdot \omega_m \cdot \underline{\psi}'_{rs}$$

$$\underline{\psi}_{ss} = L_s \cdot \underline{i}_{ss} + L_{su} \cdot \underline{i}_{r's} \quad (5b)$$

$$\underline{\psi}'_{rs} = L_{su} \cdot \underline{i}_{ss} + L'_r \cdot \underline{i}'_{rs}$$

$$M = \frac{3}{2} \cdot p \cdot Im\{\underline{i}_{ss} \cdot \underline{\psi}^*_{ss}\}$$

$$\omega_m = p \cdot \Omega_m$$

When the fluxes $\underline{\Psi}_{ss}$ and $\underline{\Psi}'_{rs}$ equations are solved, the currents $\underline{i}_{ss}$ and $\underline{i}'_{rs}$ expressions are obtained:

$$\underline{i}_{ss} = \frac{\underline{\psi}_{ss} - \frac{L_{su}}{L'_r} \cdot \underline{\psi}'_{rs}}{\sigma \cdot L_s} = \frac{1}{\sigma \cdot L_s} \cdot \underline{\psi}_{ss} - \frac{1-\sigma}{\sigma \cdot L_{su}} \cdot \underline{\psi}'_{rs} \quad (6)$$

$$\underline{i}'_{rs} = \frac{\underline{\psi}'_{rs} - \frac{L_{su}}{L_s} \cdot \underline{\psi}_{ss}}{\sigma \cdot L'_r} = \frac{1}{\sigma \cdot L'_r} \cdot \underline{\psi}'_{rs} - \frac{1-\sigma}{\sigma \cdot L_{su}} \cdot \underline{\psi}_{ss}$$

where by $\sigma = 1 - \frac{L_{su}^2}{L_s \cdot L'_r}$ is denoted *the global leakage coefficient* (*Blondel coefficient*) of induction motor.

Consequently, the linear mathematical model equations of the electromagnetic part become:

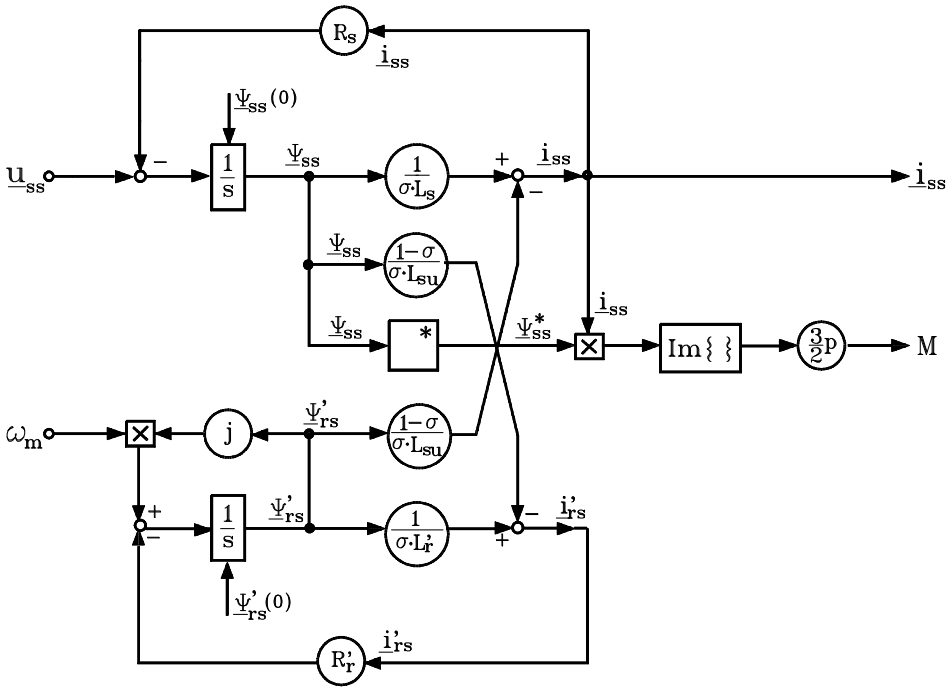

Fig.6 Structural diagram (linear model) for electromagnetic part of induction motor, with space phasors related to fixed stator referential

$$\underline{\psi}_{ss} = \int_0^t (\underline{u}_{ss} - R_s \cdot \underline{i}_{ss}) \cdot dt + \underline{\psi}_{ss}(0)$$

$$\underline{\psi}_{r's} = \int_0^t (0 - R'_r \cdot \underline{i}'_{rs} + j \cdot \omega_m \cdot \underline{\psi}'_{rs}) \cdot dt + \underline{\psi}'_{rs}(0)$$

$$\underline{i}_{ss} = \frac{1}{\sigma \cdot L_s} \cdot \underline{\psi}_{ss} - \frac{1-\sigma}{\sigma \cdot L_{su}} \cdot \underline{\psi}'_{rs} \qquad (7)$$

$$\underline{i}'_{rs} = \frac{1}{\sigma \cdot L'_r} \cdot \underline{\psi}'_{rs} - \frac{1-\sigma}{\sigma \cdot L_{su}} \cdot \underline{\psi}_{ss}$$

$$M = \frac{3}{2} \cdot p \cdot Im\{\underline{i}_{ss} \cdot \underline{\psi}^*_{ss}\}; \ \omega_m = p \cdot \Omega_m$$

On basis of equations (7), the structural diagram (linear model) of the electromagnetic part is represented in Fig.6. It is obviously that, basicly, a structural diagram represents the graphical image of the differential equations corresponding to the mathematical model of the dynamic regime of the physical system taken into account. Hence, real or complex variables are represented by lines with arrows and graphical symbols are associated to the mathematical operations effected on the variables.

The top side of the structural diagram is corresponding to the stator quantities, while in the bottom side are represented the rotor quantities. Exactly like within an ecosystem operation, between the two parts of the technical system (in our case, the induction machine) a symbiosis interconnection can be noticed as significant. The input quantity is the stator voltages space phasor $\underline{u}_{ss}$, while the output quantities are the stator currents space phasor $\underline{i}_{ss}$ and the electromagnetic torque M.

The electromagnetic torque M is acting upon the system mechanical part, which together with the mechanical transmission and the mechanical load will determine the rotor mechanical angular speed Ω_m Through the mechanical pulsation $\omega_m = p \cdot \Omega_m$, this represents *the feedback of the mechanical part reaction* on the electromagnetic part of the induction motor.

One could highlight that *a structural diagram is illustrating, according to the model of an industrial ecosystem, the interactions and the feedback loops among the different variables (currents and fluxes) which describe the induction motor operation*.

Even in the case of linear electromagnetic model, the induction motor electromagnetic part is described by a non-linear mathematical system, as it is graphical illustrated in the structural diagram by the two multiplication variables blocks. Also, it must be noticed that, excepting ω_m and M, all variables are complex quantities. They can be decomposed in the components α and β, but the resulting equations are more complex, that's why one could consider that it is better to work with the space phasors as long as it is possible.

3.2.2 Nonlinear Electromagnetic Pattern

The nonlinear electromagnetic model takes into account *the saturation of flowing paths of the main (useful) flux* Ψ_u. One could work under the assumption that the leakage fluxes (both of stator $\Psi_{s\sigma}$, and of rotor $\Psi'_{r\sigma}$) are not influenced by the main flux saturation, and can be written as the form: $\underline{\Psi}_{s\sigma} = L_{s\sigma} \underline{i}_{ss}$ and $\underline{\Psi}'_{r\sigma} = L'_{r\sigma} \underline{i}'_{rs}$, respectively.

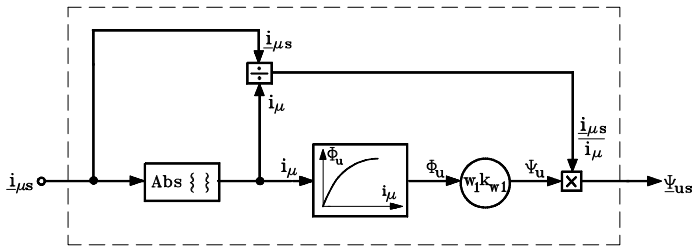

Fig.7 Magnetizing pattern of nonlinear ferromagnetic core

In this framework, and taking into account the assumptions $\omega_\lambda = 0$, $\underline{u}'_{r\lambda} = 0$ (in case of squirrel cage rotor), replacing $\lambda = s$, the equations become:

$$\underline{u}_{ss} = R_s \cdot \underline{i}_{ss} + \frac{d\underline{\psi}_{ss}}{dt}$$

$$0 = R'_r \cdot \underline{i}'_{rs} + \frac{d\underline{\psi}'_{rs}}{dt} - j \cdot \omega_m \cdot \underline{\psi}'_{rs}$$

$$\underline{\psi}_{ss} = L_{s\sigma} \cdot \underline{i}_{ss} + \underline{\psi}_{us} \qquad (8)$$

$$\underline{\psi}'_{rs} = L'_{r\sigma} \cdot \underline{i}'_{rs} + \underline{\psi}_{us}$$

$$\underline{i}_{ss} + \underline{i}'_{rs} = \underline{i}_{\mu s}; \ \psi_u = \psi_u(i_\mu)$$

$$M = \frac{3}{2} \cdot p \cdot Im\{\underline{i}_{ss} \cdot \underline{\psi}^*_{ss}\}$$

Note that due to the magnetic circuit symmetry, every induction motor will have a single magnetizing characteristic. Further on, to an induction motor by *ferromagnetic core magnetizing characteristic* one could understand the nonlinear dependence between the useful fascicular flux $\varphi_u = \varphi_1$ (corresponding to the magnetic induction base harmonic in the air gap) through a polar surface and the total current magnitude $i_\mu = |\underline{i}_{\mu s}|$. Concretely, the functional $\varphi_u = \varphi_u(i_\mu)$ could be given graphically or numerically. Also, between the useful fascicular flux magnitude $\varphi_u = \varphi_1$ and the total useful flux $\Psi_u = \Psi_{f1}$ (through the surface corresponding to all stator phase winding turns) the relation is $\Psi_u = w_1 \cdot k_{w1} \cdot \varphi_u$.

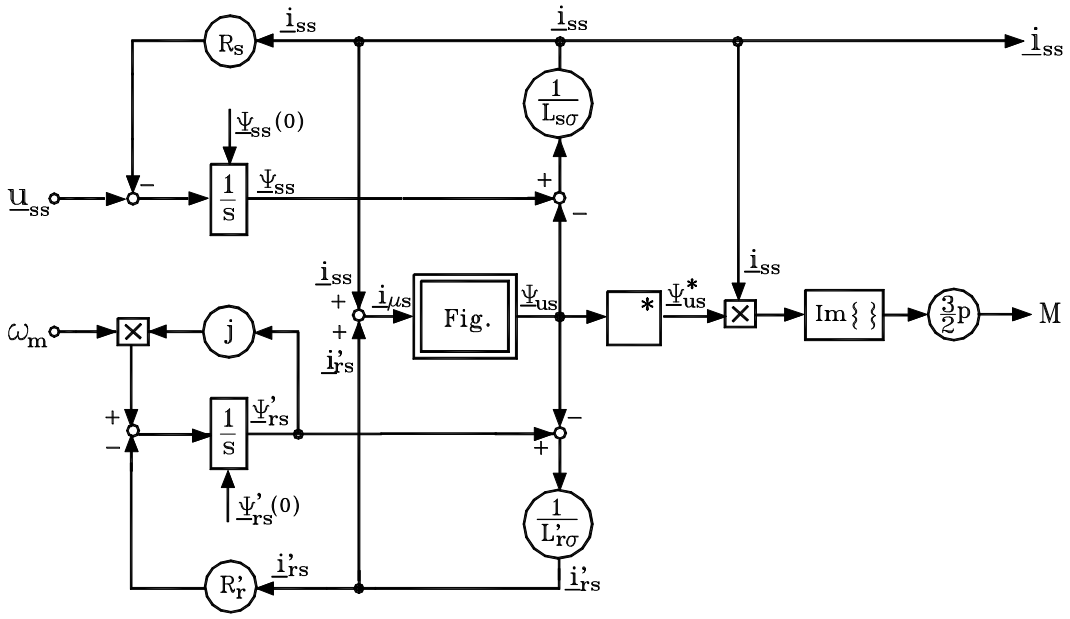

Fig.8 Structural diagram (nonlinear pattern) for electromagnetic part of induction motor, with spacephasors related to fixed stator referential

Moreover, neglecting the iron flows ($p_{Fe} = 0$), it means that the space phasors $\underline{\Psi}_{us}$ and $\underline{i}_{\mu s}$ will have the same direction (co-linear phasors) in any coordinates frame. Mathematically, the co-linearity will be expressed as below:

$$\frac{\underline{\psi}_{us}}{|\underline{\psi}_{us}|} = \frac{\underline{i}_{\mu s}}{|\underline{i}_{\mu s}|} \quad \Rightarrow \quad \underline{\psi}_{us} = \psi_u \cdot \frac{\underline{i}_{\mu s}}{i_\mu} \tag{9}$$

where: $|\underline{\Psi}_{us}| = \Psi_u$ and $|\underline{i}_{\mu s}| = i_\mu$.

Hence, the ferromagnetic core non-linearity will be described by the equations:

$$i_\mu = Abs\{\underline{i}_{\mu s}\}\ ; \quad \phi_u = \phi_u(i_\mu)$$

$$\psi_u = w_1 \cdot k_{w1} \cdot \phi_u\ ; \quad \underline{\psi}_{us} = \psi_u \cdot \frac{\underline{i}_{\mu s}}{i_\mu} \tag{10}$$

In Fig.7, for the equations as above, the model of nonlinear ferromagnetic core magnetizing it is represented as a structural diagram form.

So, taking into account the ferromagnetic core non-linearity equations, the mathematical model of the electromagnetic part can be written as the following form:

$$\underline{\psi}_{ss} = \int_0^t (\underline{u}_{ss} - R_s \cdot \underline{i}_{ss})dt + \underline{\psi}_{ss}(0)$$

$$\underline{\psi}'_{rs} = \int_0^t (0 - R'_r \cdot \underline{i}'_{rs} + j \cdot \omega_m \cdot \underline{\psi}'_{rs})dt + \underline{\psi}'_{rs}(0) \tag{11a}$$

$$\underline{i}_{ss} = \frac{\underline{\psi}_{ss} - \underline{\psi}_{us}}{L_{s\sigma}}\ ; \quad \underline{i}'_{rs} = \frac{\underline{\psi}'_{rs} - \underline{\psi}_{us}}{L'_{r\sigma}}$$

$$\underline{\psi}_{us} = \psi_u \cdot \frac{\underline{i}_{\mu s}}{i_\mu};\ \underline{i}_{\mu s} = \underline{i}_{ss} + \underline{i}'_{rs};\ i_\mu = Abs\{\underline{i}_{\mu s}\} \tag{11b}$$

$$\psi_u = w_1 \cdot k_{w1} \cdot \phi_u\ ; \quad \phi_u = f(i_\mu)$$

$$M = \frac{3}{2} \cdot p \cdot Im\{\underline{i}_{ss} \cdot \underline{\psi}^*_{ss}\} = \frac{3}{2} \cdot p \cdot Im\{\underline{i}_{ss} \cdot \underline{\psi}^*_{us}\}$$

Consequently, with the space phasor $\underline{u}_{ss}$ as input quantity and the mechanical part feedback $\omega_m = p \cdot \Omega_m$ assumed as known, in Fig.8 had been represented *the structural diagram for the electromagnetic part (in case of non-linear model) of the induction motor, with the space phasors written in the fixed referential, related to the stator*.

Further on, the validity of the structural diagrams can be demonstrated by simulations of the induction motor operation regimes using the mathematical models implementation in Matlab-Simulink.

One could record that, whatever is the analyzed pattern (a linear or a non-linear one), the structural diagram of the electromagnetic part, described with the space phasors in the stator fixed referential, does not reflect entirely the influence of the supply voltages frequency f_s (or pulsation $\omega_s = 2\pi f_s$). Looking forward, for a more close modeling as an industrial ecosystem of the induction motor behavior, one could try an analysis of the electromagnetic part described by the

space phasors related to an referential which is rotating with the synchronism speed $\omega_\lambda = \omega_s$.

4 Simulations of Three-phase Induction Machine in Dynamic Regimes

The validity and reliability of the achieved mathematical models and structural diagrams had been verified by the implementation in Matlab-Simulink. It is considered a traction induction motor MAB T_2 with the parameters presented in Table 1.

Tabel 1

No	Type	Symbol	MAB T_2 (Y)
1	Rated power [kW]	P_n	100
2	Rated voltage [V]	U_n	560
3	Rated current [A]	I_n	130
4	Starting current [A]	I_p	975
5	Rated frequency [Hz]	f_n	60
6	Variation range of supply voltage frequency [%]	D	200
7	Rated power factor	$\cos\varphi_n$	0,87
8	Poles pairs number	p	3
9	Rated speed [rot/min]	n_n	1168
10	Rated efficiency [%]	η_n	0,9
11	Motor weight [kg]	m	1250
12	Rated torque [Nm]	M_n	817,6
13	Starting torque [Nm]	M_p	899,4
14	Stator resistance [Ω]	R_1	0,0557

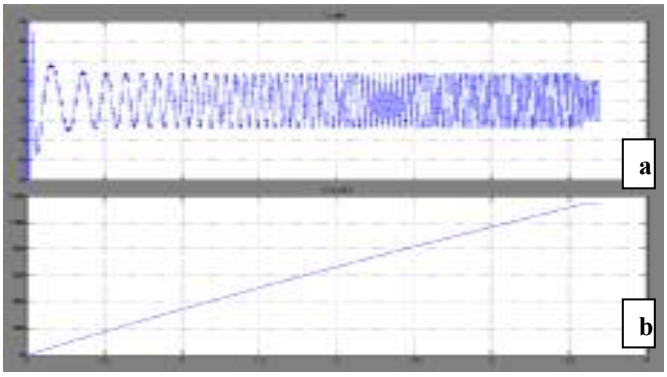

Fig.9 Transient starting regime simulation of traction induction motor supplied at variable voltage and frequency source n^*=1135 rot/min (ω^* =118,9rad/s): a) Phase current; b) Speed

In Fig.9 there are presented the simulations of phase current and speed in the transient starting regime of traction induction motor supplied at variable voltage and frequency source n^*=1135 rot/min (ω^* =118,9rad/s).

In Fig. 10 and Fig.11 there are represented in Matlab Space the main quantities waves (voltages, currents, angular speed, electromagnetic torque) for the traction induction motor MABT$_2$

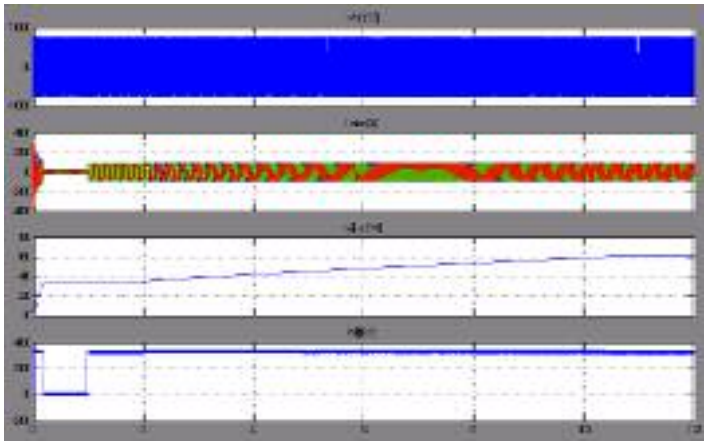

Fig. 10 Transient regime of traction motor MAB T_2 when there are modified the prescribed quatities: angular speed and resistent torque:
-at t = 0 s : ω* = 35 rad/s; Mr* = 0 Nm
-at t = 1 s : ω* = 35 rad/s; Mr* = 328,2 Nm
-at t = 2 s : ω* = 60 rad/s; Mr* = 328,2 Nm

There had been performed simulations [11] for various transient regimes of the induction motor MAB T_2, by prescribing for the drive system (basicly, the static converter and the traction motor) the different values for the angular speed and the resistent torque. Hence, in Fig.10 there are emphasized that:

- at t = 0 s there had been prescribed ω*=35 rad/s and Mr* = 0 Nm. It can be seen that after 0,15s the regime is stabilized at the prescribed value ω=35rad/s;
- at t = 1s there had been prescribed ω*=35rad/s and Mr* = 328,2 Nm. It can be noticed that the angular speed ω has no modification (ω=35rad/s);
- at t = 2s there had been prescribed ω*=60rad/s and Mr* = 328,2 Nm. It can be seen that after 8s the regime is stabilized at the prescribed value (ω=60 rad/s).

The drive system had rapidly taken the mechanical disturbances, due to the automatic speed adjustement control system. The integrative feature of the automatically regulated speed system allows a stationary error Δω = 0, and the anticipatory character of the same system affords a rapid stabilization of the real angular speed ω at the prescribed value (*), as this is reflected in the shape of the characteristic ω = f(t).

In the same manner, Fig.11 is highlighting that:
- at t = 0 s there had been prescribed ω*=30rad/s and Mr* = 328,2 Nm. It can be noticed that the regime is stabilized at the prescribed value (ω=30rad/s) after 6 seconds;
- at t = 16 s there had been prescribed ω*=50rad/s and Mr* = 328,2 Nm. It can be seen that after 5,5 s

the regime is stabilized at the prescribed value (ω=50 rad/s).

The same observation in this case must be noticed, the drive system had rapidly taken the mechanical disturbances, due to the automatic speed adjustement control system.

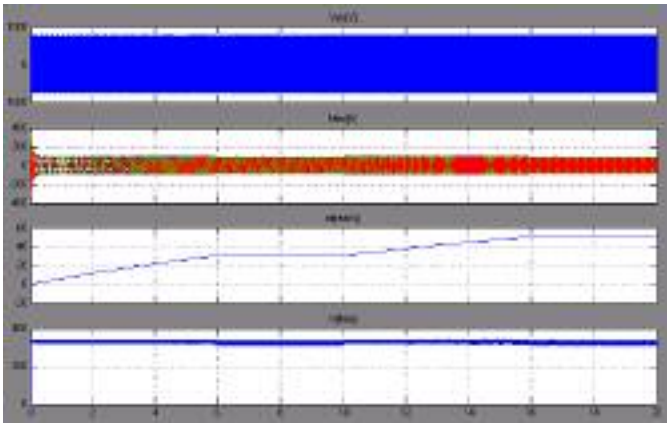

Fig. 11 Transient regime of traction motor MAB T_2 when there are modified the prescribed quatities: angular speed and resistent torque:
-at t = 0 s : ω* = 30 rad/s; Mr* = 328,2 Nm
-at t = 10 s : ω* = 50 rad/s; Mr* = 328,2 Nm

4 Conclusion

This study is an attempt to demonstrate that the conceptual framework of Industrial Ecology offers a new direction for identifying and implementing the strategies to reduce the environmental impacts of equipments and processes associated with industrial systems. The present industrial metabolism, based on Earth resources depletion and environmental destruction, should be critically reassessed from a sustainability perspective. In this paper had been pointed the ecosystem key-features suitable for the electrically driven transportation systems analysis. By modeling the electrical traction machines dynamic regimes according to an industrial ecosystem pattern, one could attempt to minimize the environmental impacts and optimize the efficiency of energy use within the transportation systems operation. The only further solution is to accept that the industry is partly the problem, as well as Science and techniques are the solution for an economical development based on an industry in harmony with the environment.

References:

[1] Allenby B.R., *Industrial Ecology: Policy Framework and Implementation*. Prentice-Hall, New Jersey, 1999.

[2] Graedel T.E. and Allenby B.R., *Industrial Ecology*. Prentice Hall, New Jersey, 1995.

[3] Nicola D.A. Cismaru D.C., *Tractiune Electrica (Electrical Traction)*, SITECH Publishing House, Craiova, Romania, 2006.

[4] Kaller R. Allenbach J.M., *Traction Electrique (Electrical Ttraction),* Vol.1,2,PPUR, Lausanne, 1995.

[5] Ayres R.U., Industrial Metabolism. In Ausubel, J.H. and Sladovich H.E. (eds): *Technology and Environment*, pp. 23-49, National Academy Press, Washington, 1989.

[6] Holling C.S., Schindler D.W., Walker B.W. and Roughgarden J., *Biodiversity in the Functioning of Ecosystems*. In Perrings, C., Maler K.-G., Folke C., Holling C. S. and Jansson B.-O. (eds), *Biodiversity Loss*, pp. 44-83, Cambridge University Press, 1995.

[7] Bulucea C. A., Nicola D.A., Brandusa C., *Assessment of Achieved Energy in Electrical Transportation Systems*, the 8th WSEAS International Conference on POWER SYSTEMS (PS'08), University of Cantabria, Santander, Spain, September 23-25, 2008, POWER SYSTEMS and POWER TECHNOLOGIES pp.164-171.

[8] Nicola D.A., Bulucea C.A., Cismaru D.C., Brandusa C.., *Energy Saving in Electric Trains with Traction Induction Motors*, The 4rth IASME/WSEAS Int. Conference on ENERGY & ENVIRONMENT, University of Cambridge, UK, February 24-26, 2009, 226-232.

[9] Klima J., *An Analytical Model and Investigation of Induction Motor Drive Fed from Three-Level Space-Vector Modulated VSI*, Proceedings of 6th WSEAS/IASME International Conference on ELECTRIC POWER SYSTEMS, HIGH VOLTAGES, ELECTRIC MACHINES (POWER'05), Tenerife, Spain, December, 2006.

[10] Mastorakis N.E., *Numerical Solution of Non-Linear Ordinary Differential Equations via Collocation Method (Finite Elements) and Genetic Algorithm*", WSEAS Transactions on Information Science and Applications, Issue 5, Volume 2, 2005, pp. 467-473.

[11] Bulucea C. A., Nicola D.A., Manolea Gh., Brandusa C., *Sustainability Concepts in Environmental and Engineering Education*, WSEAS TRANSACTIONS on ADVANCES in ENGINEERING EDUCATION, Issue 7, Volume 5, July 2008, pp.447-458, ISSN: 1790-1979.

[12] Nicola D.A., Rosen M.A., Bulucea C.A., Brandusa C., *Sustainable Energy Conversion in Electrically Driven Transportation Systems*, Proc. 6th WSEAS Int. Conf. on Engineering

Education (EE'09), Rodos (Rhodes) Island, Greece, July 22-24, 2009, 124-132.

[13] Mastorakis N.E., Bulucea C.A., Nicola D.A., *Modeling of Three-phase Induction Motors in Dynamic Regimes According to an Ecosystem Pattern,* Proc. 13th WSEAS Int. Conf. on Systems (CSCC'09), Rodos (Rhodes) Island, Greece, July 22-24, 2009, pp. 338-346, ISBN: 978-960-474-097-0, ISSN: 1790-2769.

[14] Rosen M.A., Bulucea C.A., Assessing Electrical Systems via Exergy: a Dualist View Incorporating Technical and Environmental Dimensions, *Proc. 6th WSEAS Int. Conf. on Engineering Education (EE'09)*, Rodos (Rhodes) Island, Greece, July 22-24, 2009, 116-123.

[15] Brandusa C., *Driving Systems with Static Converters and Induction Motors in Electric Urban Traction*, Ph.D. Thesis, University of Petrosani, Romania, 2007.

[16] Nicola D.A., Bulucea C.A., *Electrotechnics*, *Electrical Equipmen and Machines*, SITECH Publishing House, Craiova, Romania, 2005.